Atmospheric Environment 255 (2021) 118421

Contents lists available at ScienceDirect

Atmospheric Environment

journal homepage: www.elsevier.com/locate/atmosenv

The characteristics and size of lung-depositing particles vary significantly between high and low pollution traffic environments

Laura Salo [a,*], Antti Hyvärinen [b], Pasi Jalava [c], Kimmo Teinilä [b], Rakesh K. Hooda [b], Arindam Datta [b], Sanna Saarikoski [b], Henna Lintusaari [a], Teemu Lepistö [a], Sampsa Martikainen [a], Antti Rostedt [a], Ved Prakash Sharma [d], Md. Hafizur Rahman [d], Sanjukta Subudhi [e], Eija Asmi [b], Jarkko V. Niemi [f], Heikki Lihavainen [b,g], Banwari Lal [d], Jorma Keskinen [a], Heino Kuuluvainen [a], Hilkka Timonen [b], Topi Rönkkö [a]

[a] Aerosol Physics Laboratory, Physics Unit, Tampere University, Tampere, FI-33720, Finland
[b] Atmospheric Composition Research, Finnish Meteorological Institute, P.O. Box 503, FI-00101, Helsinki, Finland
[c] Inhalation Toxicology Laboratory, Department of Environmental and Biological Sciences, University of Eastern Finland, P.O. Box 1627, FI-70211, Kuopio, Finland
[d] Earth Sciences and Climate Change Division, The Energy and Resources Institute, New Delhi, 110003, India
[e] Advanced Biofuels Program, The Energy and Resources Institute, New Delhi, 110003, India
[f] Helsinki Region Environmental Services Authority, Helsinki, P.O. Box 100, FI-00066, Finland
[g] Svalbard Integrated Arctic Earth Observing System, P.O. Box 156, 9171, Longyearbyen, Norway

HIGHLIGHTS

- LDSA particle size distributions compared between Delhi-NCR and Helsinki.
- Particles contributing to LDSA were up to five times larger in Delhi-NCR.
- Size differences indicate different sources and different chemical composition.
- Results may explain reported discrepancies in $PM_{2.5}$ toxicity between the cities.

ARTICLE INFO

Keywords:
Air quality
Particle size distribution
Traffic emissions
LDSA

ABSTRACT

Currently, only the mass of sub 2.5 μm and sub 10 μm particles ($PM_{2.5}$, PM_{10}) in ambient air is regulated and monitored closely, but the same increase in $PM_{2.5}$ can cause different degrees of health effects in different cities (sometimes more harmful effects per unit mass in less polluted cities) (Li et al., 2019). In addition to mass concentration, other measurement metrics are needed to connect particle pollution data and health effects. In our measurements made in traffic-influenced environments in Helsinki, Finland (a relatively clean city), and Delhi-National Capital Region (Delhi-NCR), India (a polluted area), we noted a large difference in the median particle size for lung-deposited surface area (LDSA). In Helsinki, the median size was 80 nm, corresponding to soot particles emitted from diesel engines. However, the median size increased to 190 nm during a long-range transport event of air mass. In Delhi-NCR, surprisingly, the median size was even larger, 410 nm. These larger particles were likely to originate from regional sources rather than local traffic. The LDSA to $PM_{2.5}$ ratio for particles in Helsinki was 2–4 times the amount in Delhi-NCR, potentially linked with the higher toxicity of a unit of particulate mass in Helsinki.

1. Introduction

Particulate matter in urban air is one of the leading causes of premature death. Recent studies provide numbers between 3.3 and 4.2 million excess deaths annually due to ambient air pollution (Lelieveld et al., 2015; Cohen et al., 2017). The relationship between $PM_{2.5}$ and

* Corresponding author. Korkeakoulunkatu 3, 33720, Tampere, Finland.
E-mail address: laura.salo@tuni.fi (L. Salo).

https://doi.org/10.1016/j.atmosenv.2021.118421
Received 21 December 2020; Received in revised form 19 March 2021; Accepted 11 April 2021
Available online 20 April 2021

health effects has been thoroughly verified in epidemiological studies around the world (e.g. US (Samet et al., 2000), China (Lu et al., 2015; Song et al., 2017), Europe (Pelucchi et al., 2009; Lelieveld et al., 2019) and India (Balakrishnan et al., 2019)). While most studies and current regulations are based on particulate mass concentrations, the relationship between particle mass concentration and health effects differs from city to city (Li et al., 2019; Ritchie, 2019). For example, the per unit mass death rate caused by outdoor air pollution is 40% higher in Finland than in India (Ritchie, 2019). To address this issue, researchers have proposed the adoption of additional metrics like particle number concentration (e.g. (de Jesus et al., 2019)), surface area concentration (e.g. (Oberdörster, 1996; Schmid and Stoeger, 2016)), oxidative potential (OP) (Daellenbach et al., 2020) and chemical composition (e.g. (Li et al., 2019)). These metrics require new measurement techniques, as well as applying those techniques in real environments before conclusions can be made on their explanatory power.

The surface area of micro-scale particles has been foreseen as one of the main determinants of harmfulness in toxicological studies (Schmid and Stoeger, 2016; Oberdörster et al., 2005; Stoeger et al., 2006) and in lung functions (Moshammer and Neuberger, 2003). The increase in surface area of particles, compared to mass, causes more reactivity between the inhaled materials and the biological systems, leading to toxic effects (Bakand and Hayes, 2016), as well as inflammatory reactions (Keller et al., 2014). It should be noted, however, that these studies have been conducted with insoluble particles, and the results are likely to differ for soluble particles. However, not only is the surface of the particle the reaction site; toxic vapors released from emission sources can condense on surfaces, increasing the harmfulness of particles and even turning otherwise innocuous particles into harmful ones. Soluble as well as insoluble particles can act as condensation nuclei, so from this perspective the surface area of soluble particles can also be relevant when considering potential health effects of ambient aerosols.

The lung-deposited surface area (LDSA) of particles is a metric related to the abovementioned harmfulness of particulate surface area, defined as the concentration of particle surface area multiplied by a deposition function (usually alveolar deposition), which is dependent on the particle size. LDSA concentration has been shown to be a health-relevant metric in some health assessments (Patel et al., 2018; Aguilera et al., 2016). So far, only a few epidemiological studies have been published on LDSA and health effects (Patel et al., 2018; Aguilera et al., 2016; Pañella et al., 2017; Mostafavi et al., 2019; Tran et al., 2020; Habre et al., 2018). These studies have reported LDSA as a sensitive marker for lung function (Patel et al., 2018; Habre et al., 2018), atherosclerosis (Aguilera et al., 2016), cardiovascular mortality (Hennig et al., 2018), and asthma (Pañella et al., 2017; Mostafavi et al., 2019; Habre et al., 2018) as well as a good indicator of personal exposure in different environments (Tran et al., 2020). In a review of mouse and rat exposure studies, the delivered dose of particle surface area was the most relevant metric for acute lung toxicity, when comparing non-soluble spherical nanoparticles of different compositions (Schmid and Stoeger, 2016). In principle, LDSA could be used to estimate the adverse health effects of particles in ambient air, however, information on the LDSA of particles in different environments is currently very limited. This makes it impossible to fully understand the contribution of ambient particles' LDSA to diseases and premature deaths.

Atmospheric transformation processes have a significant role in the toxicity of particulate matter. The OP of particles is often used as a proxy for measuring the intrinsic toxicity of an aerosol in acellular assays. In general, smaller particles have more OP than larger particles, but OP also varies spatially (Saffari et al., 2014). A previous study reported that organic aerosol from biomass burning and cooking has a larger OP than urban background aerosol (Verma et al., 2015). It has also been shown that secondary organic aerosol (SOA) formed from gasoline engine exhaust has greater OP than primary engine emissions (Lovett et al., 2019). This suggests that the atmospheric conversion of vehicle exhaust emissions may increase OP. However, the mechanism of particulate matter (PM) toxicity is not straightforward and various toxicity mechanisms have to be considered. While SOA causes adverse health effects through inflammation and oxidative stress, it is not effective in causing cell death. The health effects of SOA might be mediated through increased particle number concentration rather than mass (Gaschen et al., 2010). A study by Park et al. (2018) investigated fresh emissions from biomass and diesel exhaust, SOA, as well as sulfate and nitrate aerosols, and found the long-aged aerosols to be less toxic. This is also supported by a previous article studying the effects of long-range transport (LRT) episodes in Helsinki (Jalava et al., 2006). It was reported that the inflammatory and cytotoxic potential of the locally produced, fresh aerosol was higher than that of LRT aerosols, indicating that after several days in the atmosphere, the toxicity of PM decreases. Previous measurements of OP in Delhi showed that OP of $PM_{2.5}$ was mainly dependent on SOA (Puthussery et al., 2020); however, OP per unit of particulate mass was low, when compared to similar measurements in Illinois, USA, where both SOA and traffic contributed to the OP (Puthussery et al., 2018).

LDSA measurements inherently include deposition into lungs, which has not been considered in past toxicological studies. New toxicological methods, such as air-liquid interface exposure of cells, can detect the effects of the whole aerosol on cell cultures (Aufderheide and Mohr, 1999; Mülhopt et al., 2016; Ihalainen et al., 2019; Ihantola et al., 2020). In these methods, the aerosol sample is directed to cells and thereafter toxicological endpoints can be measured and correlated to aerosol properties, including surface area. However, this methodology needs to be further evaluated to build a direct link to adverse health effects.

Only a few previous studies report the total LDSA concentrations measured in cities. For example, during a long-term measurement in a street canyon in Helsinki, the total LDSA was found to be 22 $\mu m^2 cm^{-3}$ on average (Kuula et al., 2020). A study in Barcelona reported a mean of 37 $\mu m^2 cm^{-3}$, and determined that particles between 50 and 200 nm contributed the most (Reche et al., 2015). There is a single previous study which reports on LDSA size distributions in various locations in Helsinki, Finland (Kuuluvainen et al., 2016). The highest particle mode at traffic sites was at around 100 nm, corresponding to fresh vehicle emissions (Kittelson, 1998), while a residential suburban area had the highest mode at 200–300 nm.

In this study, we employed a recently developed method to measure LDSA as a function of particle size over a large size range of particles (Lepistö et al., 2020). Measurements were conducted at two contrasting measurement sites: Helsinki, Finland and Delhi-NCR, India. Both measurement sites were in the immediate vicinity of busy roads with similar traffic rates. Our main aim was to characterize the differences in LDSA size distributions between the relatively clean traffic environment (Helsinki) and the very polluted traffic environment (Delhi-NCR).

2. Material and methods

2.1. Measurement locations

This study consisted of two measurement campaigns that were both conducted in roadside environments, the first in Delhi-NCR, India, and the second in Helsinki, Finland. The exact locations of the measurement sites are shown in Fig. 1. In Helsinki, we were able to use an existing long-term measurement site, and in Delhi-NCR we used a mobile laboratory to house the instruments close to the road.

Helsinki is a coastal city in the Southern region of Finland, north of the Baltic sea with a population of 650 000 (Population, 2019). The air quality in Helsinki is relatively good on average (Pohjola et al., 2002; Virtanen et al., 2006; Pirjola et al., 2017). In 2019, the $PM_{2.5}$ concentration did not exceed WHO guidelines (yearly average below 10 $\mu g/m^3$) at any of 11 measurement locations (Korhonen et al., 2020). The Helsinki measurements were conducted at the HSY supersite (60°11′N, 24°57′E), operated by Helsinki Region Environmental Services Authority (HSY). The supersite was on the south-west side of the road, which

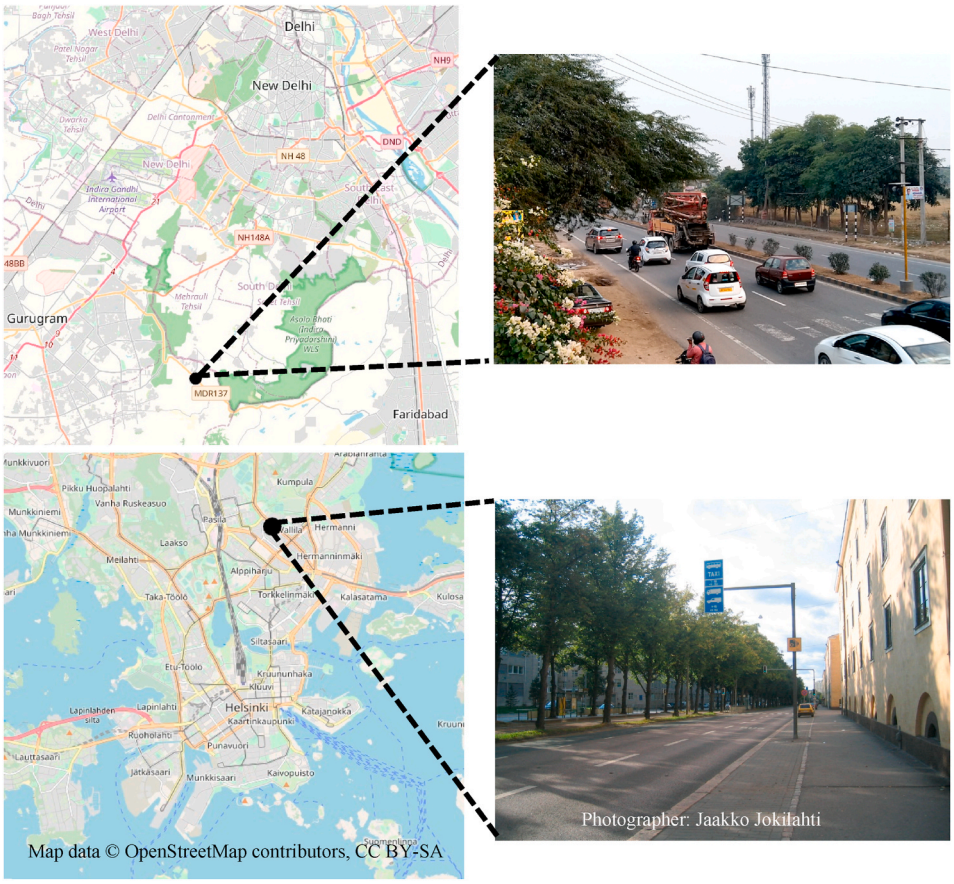

Fig. 1. Measurement locations marked with a black dot in Delhi-NCR (top) and Helsinki (bottom).

has three lanes going both ways, separated by trees, and a tram-railway in between. The surroundings are described in more detail in Kuuluvainen et al. (2018). Our study was conducted during a rather warm period (temperatures between 10 and 20 °C) in the beginning of September 2019. During that time, the most significant local particle source was traffic of the closest road, with 1167 vehicles/hour, 10% of which were heavy-duty (information from City of Helsinki).

The measurement site in India was in Gwal Pahari, on the south border of Delhi-NCR (28°43′N, 77°15′E), along a busy road with two lanes in both directions. The measurements were conducted during November and December of 2018. The ambient temperature varied between 8 °C to 20 °C during the period. The area is located approximately 20 km southward from the center of Delhi, which is one of the largest cities in the world, with an estimated population of 29 million in 2018 (Delhi and India Population, 2019). It is in the Indo-Gangetic Plain in northern India. Many studies report on the air quality and meteorology in the area (Nair et al., 2007; Hyvärinen et al., 2010; Tiwari et al., 2013; Joshi et al., 2016). $PM_{2.5}$ pollution is usually high (Raatikainen et al., 2014), especially during the winter (for example, the average $PM_{2.5}$ measured in 2011 was over 300 μg/m^3 for December) (Tiwari et al., 2013). Deaths due to poor air quality in India have been increasing between 1998 and 2015, especially in North India (Jia et al., 2020). The diurnal variation during winter is affected by the planetary boundary layer, which heightens during the day, leading to the dilution of polluting components (Nair et al., 2007; Hyvärinen et al., 2010; Tiwari et al., 2013). To the north-east of the measurement site there was a golf course and a green area, and in the south-west direction a road connecting Gurugram and Faridabad. Across the road was a busy street. The average traffic rate was 843 vehicles/hour and 7.5% of those were heavy-duty. The traffic count was done in March 2019 (spring after the measurement campaign) by hand and was limited to daytime traffic.

In Helsinki, the campaign instruments were housed next to a permanent measurement site, inside a shipping container. The sampled air came from inlets through the container roof, at a height of about 2.5 m. In Delhi NCR, instruments were housed in a mobile measurement laboratory. Again, the inlet was through the roof of the van, at a height of approximately 2.5 m. Due to the highly polluted air in Delhi NCR, we used a $PM_{2.5}$ impactor inlet to remove coarse particles and avoid clogging instruments. In all the presented results, the size distribution data has been limited to 2.5 μm from both measurement sites.

2.2. Instrumentation

Measurements in both locations used the same instrumentation: an ELPI+ (Electrical Low Pressure Impactor (Keskinen et al., 1992; Marjamäki et al., 2000; Järvinen et al., 2014), Dekati) to measure particle size distributions, a Quadrupole-ACSM or ToF-ACSM (Time-of-Flight Aerosol Chemical Speciation Monitor (Fröhlich et al., 2013), Aerodyne Research Inc.) to measure particle chemistry and an aethalometer (Magee Scientific, type AE31) for particle light absorption and black carbon. Both sites also had instrumentation for measuring basic meteorological data (data presented in Fig. S1 and Fig. S2). For Helsinki we have also included data from a nearby weather station (Pasila, measurement from a rooftop at 53 m above ground), as wind direction and speed below building height are influenced by the canyon geometry and passing traffic. Detailed information on each instrument is included in the Supplementary material.

2.3. Calculating LDSA

LDSA is the particle surface area multiplied by a size-dependent deposition function describing the efficiency of deposition into the

alveolar region. Most often the deposition function used is based on data from an ICRP (International Commission on Radiological Protection) model (Human respiratory tract m, 1994) which has been formulated into an empirical equation by Hinds (1999). The current from particles in the size range 30 nm–300 nm charged by a diffusion charger have a roughly linear relationship with LDSA, and this relationship is used in some sensor-type aerosol measurement devices (Fierz et al., 2014). Because the ELPI+ separates particles into bins based on their aerodynamic size, it can be used to transform the current of diffusion-charged particles into LDSA for a much larger particle size range. Instead of using just one coefficient, a coefficient can be applied to each impactor stage separately. The coefficients used in this paper use the method reported by Lepistö et al. (2020). The stage-specific values for three different effective densities of particles are presented in Table 1. Unit density is used in this article, excluding one section where the dependency of LDSA distributions on effective density is examined.

For data analysis of Delhi-NCR measurements we chose the most reliable ELPI+ data from our measurements, the first 48 h after cleaning the instrument. Because the ELPI+ collects particles, the accumulation of particles can change the response functions. This can be seen in Fig. S3, which shows the full measurement data from Delhi-NCR. We used greased aluminum foils for particle collection and, to extend the measurement period between instrument maintenance, the sample was diluted with clean air using one-to-one dilution ratio. In future long-term measurements in polluted areas, sintered collection plates could make maintenance-free measurement periods longer.

3. Results and discussion

3.1. LDSA concentrations

Fig. 2 shows the time resolved particle LDSA size distributions from the measurement locations in Delhi-NCR and Helsinki. The variation in LDSA concentrations was significant in both locations; however, it should be noted that, overall, the average LDSA concentrations were more than ten times higher in Delhi-NCR (329 ± 127 $\mu m^2/cm^3$) than in Helsinki (27 ± 15 $\mu m^2/cm^3$) and much larger than LDSA concentrations observed in previous ambient studies (Cheristanidis et al., 2020).

Although the LDSA concentrations in Helsinki were relatively low, an increase in LDSA concentration and mean LDSA size (Fig. 2 and Fig. 3) was observed between September 9th to 11th. During this period, PM mass and sulfate concentrations (Fig. S4, Fig. S5, Fig. S6) were also higher than usual. This coincided with an LRT pollution episode in Helsinki, confirmed by $PM_{2.5}$ increases also observed in background stations. Based on air mass trajectories, the pollution during the LRT period originated from central Europe and Russia (Fig. S7). Several LRT episodes are observed in Helsinki every year and their contribution to particulate mass concentrations of ambient air can be substantial (Niemi et al., 2009). Compared to this study, earlier studies (Timonen et al., 2008; Teinilä et al., 2019) have reported relatively similar changes in PM mass, composition and size distribution during LRT episodes. In this study, the LRT episode affected the data interpretation and presentation so that we divided the measurement period in Helsinki to two parts, one describing the situation dominated by local sources (later referred to as Helsinki Local) and the other describing the situation when the air quality was significantly affected by LRT aerosol (later referred to as Helsinki LRT).

The mean, minimum, maximum, and standard deviation of hourly averaged values for $PM_{2.5}$, LDSA, and mass concentration measured in Delhi-NCR and Helsinki are presented in Table 2, together with black carbon (BC) concentrations. The total BC time series are presented in Fig. S8. For the measurements in Helsinki, values are presented separately for Helsinki Local and Helsinki LRT. Although both measurements were made in roadside environments with relatively similar traffic rates on the adjacent roads (1167 vehicles/hour in Helsinki and 843 vehicles/hour in Delhi-NCR), extremely large differences were seen in LDSA concentrations. While the mean LDSA concentration in Helsinki was 27 $\mu m^2/cm^3$ and 40 $\mu m^2/cm^3$ during Helsinki Local and Helsinki LRT, respectively, the mean LDSA concentration in Delhi-NCR was 329 $\mu m^2/cm^3$. Regarding the variation of the LDSA concentrations, even the minimum hourly averaged LDSA concentration in Delhi-NCR (114 $\mu m^2/cm^3$) was larger than the mean LDSA concentrations in Helsinki. These differences were linked to concentrations of $PM_{2.5}$ and BC, which were also significantly higher in Delhi-NCR.

In addition to total LDSA concentrations, Table 2 shows the mean LDSA concentrations separately for particle size ranges of 10–30 nm, 30–150 nm and 150 nm - 2.5 μm. In this paper we will also use the terms nucleation, soot and accumulation mode for these three size ranges, as those modes can be seen in the size distributions (Fig. 3). Based on the numbers in Table 2, there were large differences in how different particle size ranges contributed to total LDSA. In Delhi-NCR, 78% of the total LDSA concentrations was from the largest size range (150 nm - 2.5 μm), whereas in Helsinki LRT data the contributions of size ranges 30–150 nm and 150 nm - 2.5 μm were more equal (38% and 50% of the total LDSA concentration, respectively). Furthermore, in Helsinki Local the dominating size range was 30–150 nm with 59% contribution to the total LDSA of ambient particles. Importantly, the variation of contributions of different particle size ranges led to differences in the LDSA to $PM_{2.5}$ ratio, which varied from 1.2 $\mu m^2 m^3/cm^3 \mu g$ in Delhi-NCR to 2.1 in Helsinki LRT and 4.5 in Helsinki Local.

The diurnal variation of the LDSA was different in the studied locations (Fig. S9); while in Helsinki no clear trend was observable, in Delhi-NCR the lowest LDSA concentrations were repeatably observed between 11 a.m. and 5 p.m. The same day-night variation has been observed in previous studies on particle mass concentrations during wintertime in Delhi-NCR and is likely a result of the aerosol diluting due to the planetary boundary layer heightening (Raatikainen et al., 2014; Hooda et al., 2016; Wang et al., 2020).

3.2. Comparison of particle number, mass and LDSA size distributions

Fig. 3 shows the average particle size distributions for particle number (left), lung-deposited surface area (middle) and particle mass (right) for Delhi-NCR, Helsinki Local and Helsinki LRT. In the Helsinki data, the LRT episode is separated as it clearly represents a different PM source, and the size distributions for the LRT episode are different from the local distribution for each metric, and especially for LDSA.

The observed particle number concentrations and size distributions for Helsinki and Delhi-NCR were relatively similar, with a maximum concentration in nucleation mode particles, and a smaller peak in soot mode particles. However, larger differences were observed for LDSA and mass size distributions. For Helsinki (local) the LDSA maximum was in the soot mode (median particle size 80 nm) and in Delhi-NCR in the accumulation mode (median particle size 410 nm). The maximum in PM

Table 1
Stage-specific coefficients used to calculate LDSA from current in the ELPI+ instrument.

		Stage													
		1	2	3	4	5	6	7	8	9	10	11	12	13	14
ρ (g/cm^3)	0.7	0.030	0.049	0.051	0.042	0.032	0.032	0.049	0.091	0.174	0.268	0.317	0.308	0.283	0.226
	1.0	0.020	0.042	0.052	0.048	0.037	0.031	0.041	0.077	0.150	0.245	0.290	0.282	0.240	0.192
	1.5	0.011	0.032	0.048	0.052	0.044	0.033	0.035	0.062	0.125	0.218	0.262	0.255	0.214	0.159

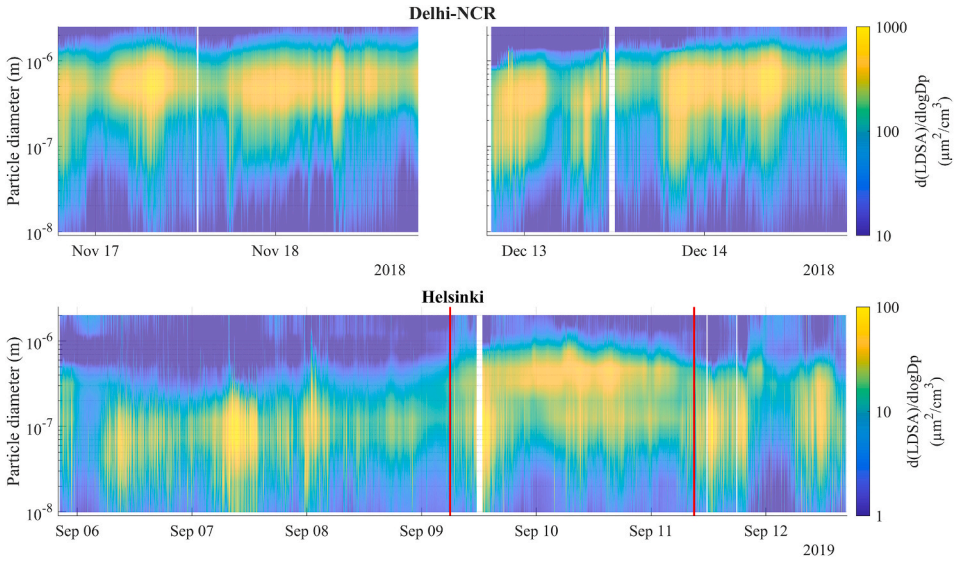

Fig. 2. LDSA size distributions for the measured time periods in Delhi-NCR and Helsinki, averaged minutely. Note the order of magnitude difference in the scales of the color bars. The Delhi-NCR time series here is relatively short but it is representative of the observed overall concentrations in Delhi-NCR during wintertime. Due to the gradual instrument overloading in the Delhi-NCR measurements, a full hourly averaged time series for LDSA is shown only in Fig. S3. The vertical red lines in the lower panel show the duration of the LRT episode.

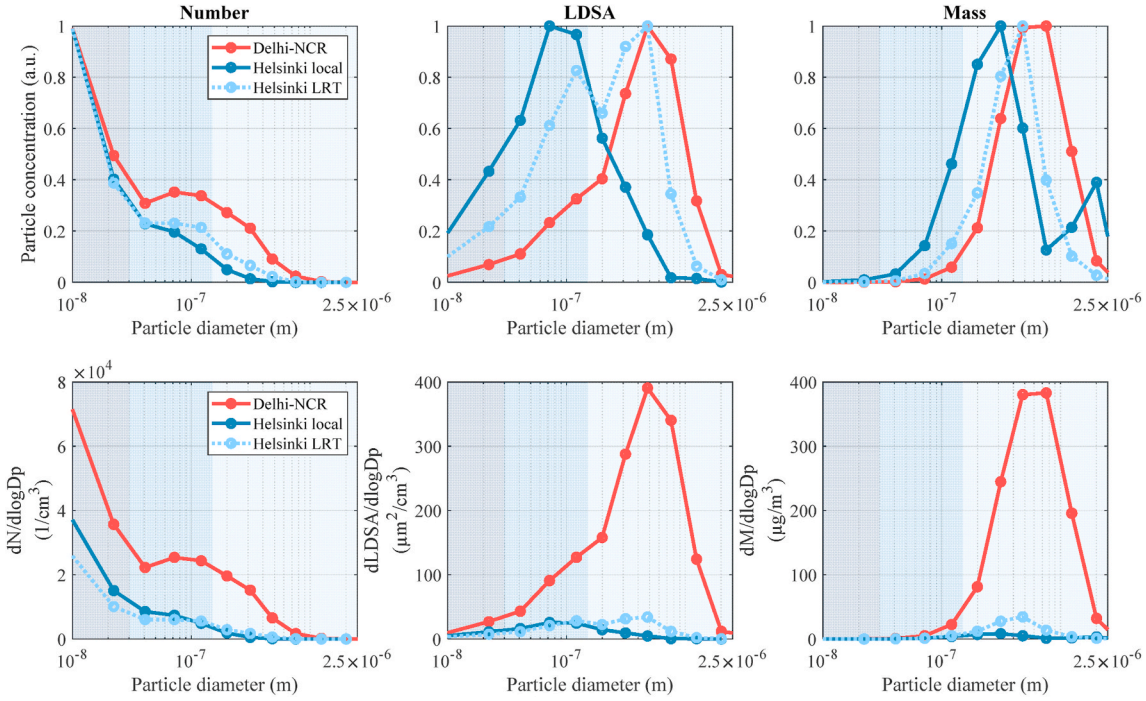

Fig. 3. Average particle size distributions for number, LDSA and mass concentrations. In the upper panel, the size distributions are normalized by dividing by the maximum value, and in the lower panel the absolute concentrations are shown. Each column represents a different moment of the distribution (number, LDSA and mass). The x-axis has been divided into three particle size bins, representing the nucleation, soot, and accumulation mode particles. For tracheobronchial and head airway deposition-weighted surface areas see Fig. S10.

Table 2
Mean, minimum, maximum, and standard deviation of hourly averaged values for PM2.5, LDSA, and BC measured in Delhi-NCR and Helsinki.

	Delhi-NCR				Helsinki Local				Helsinki LRT			
	Mean	Min	Max	Std	Mean	Min	Max	Std	Mean	Min	Max	Std
$PM_{2.5}$ (μg/m^3)	268	81	607	114	6	1	18	3	19	7	30	6
LDSA (μm^2/cm^3)	329	114	737	137	27	9	82	15	40	17	146	20
LDSA 150 nm - 2.5 μm (μm^2/cm^3)	257	85	581	108	6	0	21	4	20	8	33	6
LDSA 30 nm–150 nm (μm^2/cm^3)	60	13	178	40	16	3	65	11	15	7	92	13
LDSA 10 nm–30 nm (μm^2/cm^3)	12	1	34	8	5	1	18	4	4	1	21	4
$LDSA/PM_{2.5}$ (μm^{2}m^3/cm^{3}μg)	1.2				4.5				2.1			
BC (μg/m^3)	15.1	2.6	42.6	9.0	1.1	0.0	16.7	1.7	1.4	0.0	8.1	1.2

mass size distributions were in the accumulation mode both cases; however, the median particle size for Delhi-NCR was slightly larger (580 nm in Delhi-NCR compared to 280 nm in Helsinki). During the LRT episode, the LDSA size distribution in Helsinki became bimodal: in addition to the soot mode particles, an accumulation mode clearly appeared in the LDSA size distribution. This larger mode during the LRT episode was in a similar size range to the accumulation particle mode of the LDSA size distribution observed in Delhi-NCR. The particle size distributions for number, LDSA and mass in Helsinki are relatively similar to size distributions previously measured in Helsinki traffic environments (Kuuluvainen et al., 2016; Enroth et al., 2016). Indications of a bimodal LDSA size distribution during the LRT period have been seen in a previous study (Pirjola et al., 2017), but here the shape is very clear.

The side-by-side comparison of the different particle size distributions in Fig. 3 highlights the dependency of measurement results on the chosen metric. The number distribution emphasizes the small particles, and the mass distribution emphasizes the large particles. The LDSA distribution falls somewhere in between and shows the largest difference between the two measurement sites.

In the Delhi-NCR results, the LDSA concentration in the soot mode, representing local and fresh emissions of traffic (see e.g. (Rönkkö and Timonen, 2019)), was small in comparison to accumulation mode particle concentrations, which typically represents more aged particles, grown by condensation and coagulation, or originating from biomass combustion. In contrast, the accumulation mode particle concentration for LDSA was very small in Helsinki when the particles were from local sources; however, during the LRT event the soot mode and accumulation mode particle concentrations were approximately equal. Somewhat surprisingly, Delhi-NCR only had approximately twice the number concentration of sub 30 nm particles compared to Helsinki, partially due to the prevalence of condensation sinks in ambient air (i.e. vapors condense onto previous particles, rather than going through nucleation) and the similar amount of vehicles, which are a major source of nano-sized particles (Rönkkö et al., 2017). These smallest particles from nearby sources were therefore not the key factor for differences in the pollution levels of the studied environments during our measurement period.

Fig. 4 shows the LDSA versus mass concentration for particles in the above-mentioned three particle size groups (10–30 nm, 30–150 nm, and 150 nm - 2.5 μm), along with best-fit lines. In Delhi-NCR, the total LDSA and mass concentrations of particles are highly correlated ($R^2 = 0.81$) with close to a 1-to-1 ratio; thus, using either metric would yield the same result, i.e., a doubling of particle mass also doubles the LDSA concentration. In Helsinki local, there was almost no correlation between the $PM_{2.5}$ and total LDSA concentration—an increase in particle mass concentration can have almost no effect on total LDSA or vice versa.

As seen in Fig. 4, the slopes of correlation plots differ significantly between the measurement sites and between the chosen particle size ranges. In general, in Helsinki the increase of $PM_{2.5}$ causes a much larger relative increase of total LDSA than in Delhi-NCR; the slopes of the correlation plots between the total LDSA and $PM_{2.5}$ were 1.2 in Delhi-NCR, 2.0 in Helsinki LRT, and 3.4 in Helsinki Local. These values clearly demonstrate the differences between the studied environments, and they can explain why the ambient $PM_{2.5}$ has been observed to be more dangerous for human health in Helsinki than in Delhi (Ritchie, 2019). Furthermore, this result demonstrates that the monitoring of ambient particle LDSA and especially the particle LDSA size distributions could significantly improve the explanatory power of air quality monitoring regarding the harmful effects of particulate pollution on human health. For instance, the effect of LRT events on health in Helsinki may therefore be *less* severe than one might expect by simply observing an increase in particle mass concentration.

In addition to concentrations and lung-deposition efficiencies of the particles, the health impacts of the particles likely depend on the physical and chemical characteristics of the particles. These characteristics can vary significantly as a function of particle size and depend on the prevailing particle sources, and they likely affect the toxicity and e.g. the above-mentioned oxidative potential of the particles. Fig. 5 summarizes how the results of this study relate to particle composition and sources in an urban traffic environment. In the Figure, the LDSA and mass size distribution modes measured in our study are represented by the horizontal bars at the bottom part of the figure, showing that the soot mode size range dominate the LDSA in Helsinki but the accumulation mode size range dominates the LDSA in Delhi-NCR and, in addition, that

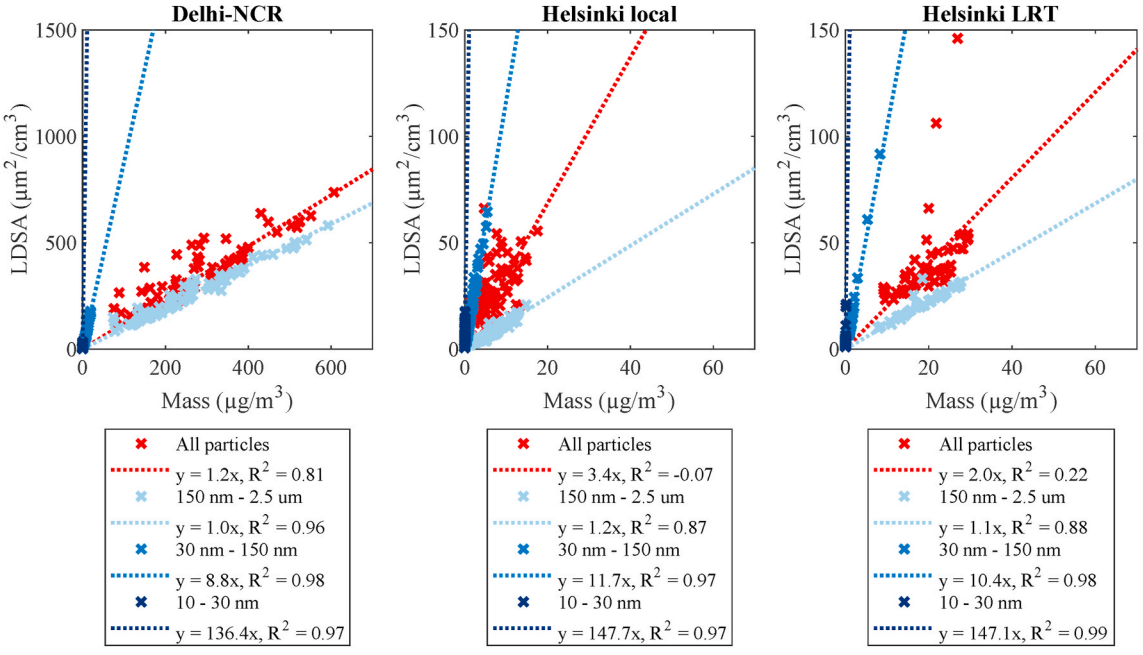

Fig. 4. Correlation plots of LDSA vs mass concentration for different particle size bins. The different colors represent the different size groups, and a best fit line has been calculated for each group, equations listed in the legend. Note the different axes used in the subfigures. (For interpretation of the references to color in this figure legend, the reader is referred to the Web version of this article.)

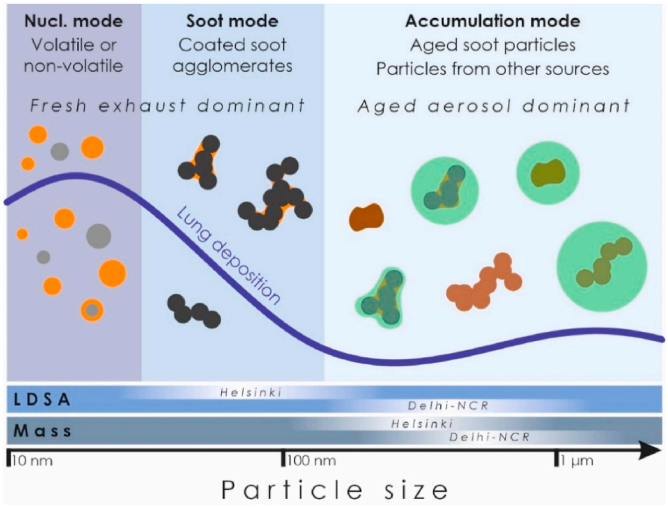

Fig. 5. Schematic of traffic environment particle types in different sizes and their lung-deposition probability. The blue lung-deposition curve shows that small particles have the highest lung deposition probability, but deposition probability increases again around 1 μm. The largest surface area of lung-depositing particles in Helsinki (Local) belongs to the medium particle size range (30–150 nm), while in Delhi NCR the largest LDSA of particles belongs to the largest particle size range (150 nm–2.5 μm), these are shown by the lighter color intensity in the LDSA strip towards the bottom. (For interpretation of the references to color in this figure legend, the reader is referred to the Web version of this article.)

the accumulation mode size range dominates the particulate mass concentrations both in Helsinki and in Delhi-NCR. These size ranges, i.e., the nucleation mode size range, soot mode size range and the accumulation mode size range, are shown in the figure as separate parts, overlaid with the bi-modal alveolar lung-deposition curve. The Figure also shows the different particle types dominating each size range. The first size range (<30 nm) is dominated by nucleation mode particles from precursor gases or tiny solid particles emitted directly from engines (Rönkkö et al., 2017). The second size range is affected mainly by freshly emitted soot agglomerates from combustion. This soot can be coated with harmful substances, such as oxidative species or polycyclic hydrocarbons (PAHs) (Biswas et al., 2009; Surawski et al., 2011). The largest particles, referred to here as the accumulation mode particles, consist typically of more aged particles, which can originate from distant sources, and e.g. biomass burning can contribute their concentrations (Tissari, 2008; Obaidullah et al., 2012). Some road dust can also be found in this size range (Zhao et al., 2017; Wang et al., 2005). Due to their different physical and chemical characteristic, particles in different size ranges can have different effects on human health, which should also be taken into account in air pollution monitoring and pollution mitigation actions.

3.3. Sources of uncertainty in the LDSA results

In this study, we assumed particles to be spherical with unit density, and to not grow due to hygroscopicity when entering the lungs. These assumptions were required to conduct the analyses above, but they led to some uncertainties in the results, as discussed below.

Many studies report on the effective densities of urban ambient particles, for example, a study at a Helsinki traffic site gives soot mode particles an effective density of 1.5 g/cm^3 in the summertime (Virtanen et al., 2006). Another study conducted at a street canyon in Copenhagen (Rissler et al., 2014) found 75 nm particles grouped into two categories of effective density: approximately 1 g/cm^3 and 1.5 g/cm^3, with the higher density particles identified as LRT aerosol, and the lower density as locally emitted soot. In the same study, particles sized 350 nm contained some very low-density soot agglomerates (0.3 g/cm^3) but were mostly LRT aerosol with a density close to 1.5 g/cm^3. Considering these previous studies, perhaps a density between 1.0 and 1.5 g/cm^3 is closer to the true mean densities of the ambient aerosols studied here. To examine the effects of density on the LDSA distribution, we calculated two additional distributions for the Delhi-NCR, Helsinki Local and Helsinki LRT data sets (Fig. S11). Assuming a higher density decreased the LDSA of accumulation mode particles, while increasing the LDSA of soot mode particles. Overall, increasing the effective density from 1.0 to 1.5 g/cm^3 did not significantly affect the total LDSA, but the relative importance of local emissions increased.

Highly fractal particles have a larger surface area than corresponding spherical particles, but they are also charged more efficiently by the diffusion charger in the ELPI+ (Ouf and Sillon, 2009)—in that sense the surface area is expected to be somewhat accurately represented. From a deposition perspective, a fractal particle is less likely to deposit by impaction, but more likely to deposit by diffusion than its counterpart sphere of equal mobility. In a previous study, the relative standard error for soot particle deposition was 1.2–3.8% when taking into account uncertainties in both shape and effective density (Vu et al., 2018).

Hygroscopicity determines how much a particle grows due to water uptake in a humid environment. Lungs have high humidity, and thus the hygroscopicity of particles is important in determining their lung-deposition fraction. Vehicle exhaust particles are mostly hydrophobic (Henning et al., 2012), but accumulation mode particles can be hygroscopic (Swietlicki et al., 2008). In our study, the effect of including hygroscopicity into calculations would likely be to increase the fraction of depositing accumulation mode particles in both Helsinki (LRT period) and Delhi-NCR, assuming that the soot mode particles are hydrophobic.

Finally, as was noted in the introduction, particle surface area has been shown to be a health-relevant metric for insoluble particles, but studies with soluble particles have not yet been conducted. Typically, in the ambient atmosphere approximately 30–60% of submicron particulate matter consist of organic compounds, 30–40% of inorganic ions and 5–20% of black carbon, depending on the particle sources and aging stage of particles (e.g. (Jimenez et al., 2009; Gani et al., 2019; Barreira et al., 2020)). Black carbon is water insoluble, approximately 50% of organic mass is water-soluble (e.g. (Timonen et al., 2010)) and inorganic ions are mostly water-soluble. Thus, the ambient aerosol contains both insoluble and soluble compounds forming as a complex internally and externally mixed aerosol. Due to that, results for ambient aerosol cannot be directly compared to laboratory studies made with purely water insoluble particles, when evaluating the potential health effects of the studied aerosols.

4. Conclusions

In this study, we conducted experiments in a relatively clean traffic environment and in a highly polluted traffic environment, i.e., in Helsinki and in Delhi-NCR. We focused the experiments on the lung-depositing surface area (LDSA) of ambient particles, aiming to understand the differences in LDSA concentrations and size distributions between the measurement sites. We observed vast differences in LDSA, both in the LDSA concentrations and in particles' LDSA size distributions. The LDSA of particles in Helsinki was mostly in the size range of the freshly emitted soot particles, but during the LRT event a second mode appeared in the larger particles. In Delhi-NCR, only a small fraction of the LDSA came from freshly emitted particles, but for most of the measurement period the larger, aged particles contributed an overwhelming majority of the LDSA, despite the lower lung deposition probability of larger particles (Fig. 5). Additionally, The LDSA to mass ratio of particles was significantly smaller in Delhi-NCR than in Helsinki, which may be one reason for the previously observed location-based differences in toxicity of ambient particulate matter (Li et al., 2019; Ritchie, 2019).

Our study indicates that if health effects of particulate pollution were

estimated based on PM mass only, they would be significantly different than if information on particle number and LDSA size distributions are considered, and further, the largest differences in this study were observed specifically in the LDSA distributions.

Here, we presented the first measured evidence that the size of lung-deposited particles differs on average by a factor of five between clean and polluted traffic environments. This implies that particle sources and expected health implications are different as well. Further toxicological and epidemiological studies along with long-term LDSA measurement data in several locations across the globe are needed to establish the detailed relationship between health and LDSA.

CRediT authorship contribution statement

Laura Salo: Data curation, Formal analysis, Measurements were designed, The measurements were conducted, Data was analyzed, The manuscript was initially written. **Antti Hyvärinen:** Measurements were designed, The measurements were conducted. **Pasi Jalava:** The manuscript was initially written. **Kimmo Teinilä:** The measurements were conducted. **Rakesh K. Hooda:** Measurements were designed, The measurements were conducted. **Arindam Datta:** The measurements were conducted. **Sanna Saarikoski:** Data curation, Formal analysis, Data was analyzed. **Henna Lintusaari:** Measurements were designed, The measurements were conducted. **Teemu Lepistö:** Data curation, Formal analysis, The measurements were conducted, Data was analyzed. **Sampsa Martikainen:** The measurements were conducted. **Antti Rostedt:** The measurements were conducted. **Ved Prakash Sharma:** The measurements were conducted. **Md. Hafizur Rahman:** The measurements were conducted. **Sanjukta Subudhi:** Measurements were designed. **Eija Asmi:** Measurements were designed. **Jarkko V. Niemi:** Measurements were designed. **Heikki Lihavainen:** Measurements were designed. **Banwari Lal:** Measurements were designed. **Jorma Keskinen:** Measurements were designed. **Heino Kuuluvainen:** Measurements were designed, The measurements were conducted, The manuscript was initially written. **Hilkka Timonen:** Measurements were designed, The manuscript was initially written. **Topi Rönkkö:** Measurements were designed, The manuscript was initially written, further discussed, edited and commented on by all authors.

Declaration of competing interest

The authors declare that they have no known competing financial interests or personal relationships that could have appeared to influence the work reported in this paper.

Acknowledgements

This work was in part funded by TAQIITA: Traffic and air quality in India: technologies and attitudes. TAQIITA project has received funding from Business Finland, Neste, Dekati, Pegasor and Helsinki Region Environmental Services Authority (HSY). TAQIITA grant number 2763/31/2015.

This work was also funded by TUBE: Transport-derived ultrafines and the brain effects. TUBE has received funding from the European Union's Horizon 2020 research and innovation program under grant agreement No 814978.

Academy of Finland Flagship funding Atmosphere and Climate Competence Center, ACCC (grant no. 337552, 337549) is gratefully acknowledged.

Laura Salo thanks the Doctoral School of Tampere University of Technology for providing a four-year salary for doctoral studies.

We wish to thank the Indian Oil Corporation Ltd., Research and Development, in Faridabad for the use of their mobile measurement laboratory along with its instrumentation and for the hard work put into overseeing the laboratory for the duration of the measurements.

We also wish to thank Mr. Matthew Bloss for his work on measurements in Gwal Pahari.

Appendix A. Supplementary data

Supplementary data to this article can be found online at https://doi.org/10.1016/j.atmosenv.2021.118421.

References

Aguilera, I., Dratva, J., Caviezel, S., Burdet, L., De Groot, E., Ducret-Stich, R.E., et al., 2016. Particulate matter and subclinical atherosclerosis: associations between different particle sizes and sources with carotid intima-media thickness in the SAPALDIA study. Environ. Health Perspect. 124 (11), 1700–1706.

Aufderheide, M., Mohr, U., 1999 Nov. CULTEX–a new system and technique for the cultivation and exposure of cells at the air/liquid interface. Exp Toxicol Pathol Off J Gesellschaft fur Toxikologische Pathol 51 (6), 489–490.

[Internet] Bakand, S., Hayes, A., 2016 Jun 14. Toxicological considerations, toxicity assessment, and risk management of inhaled nanoparticles [cited 2020 Apr 21] Int. J. Mol. Sci. 17 (6), 929. Available from: http://www.mdpi.com/1422-0067/17/6/929.

[Internet] Balakrishnan, K., Dey, S., Gupta, T., Dhaliwal, R.S., Brauer, M., Cohen, A.J., et al., 2019 Jan 1. The impact of air pollution on deaths, disease burden, and life expectancy across the states of India: the Global Burden of Disease Study 2017 [cited 2020 May 29] Lancet Planet Health 3 (1), e26–39. Available from: http://www.ncbi.nlm.nih.gov/pubmed/30528905.

Barreira, L.M.F., Helin, A., Aurela, M., Teinilä, K., Friman, M., Kangas, L., et al., 2020. In-depth characterization of submicron particulate matter inter-annual variations at a street canyon site in Northern Europe [Internet] Atmos. Chem. Phys. Discuss. 2020, 1–34. Available from: https://acp.copernicus.org/preprints/acp-2020-908/.

Biswas, S., Verma, V., Schauer, J.J., Cassee, F.R., Cho, A.K., Sioutas, C., 2009 May 15. Oxidative potential of semi-volatile and non volatile particulate matter (PM) from heavy-duty vehicles retrofitted with emission control technologies [Internet] Environ. Sci. Technol. 43 (10), 3905–3912. https://doi.org/10.1021/es9000592. Available from:

Cheristanidis, S., Grivas, G., Chaloulakou, A., 2020 Sep. Determination of total and lung-deposited particle surface area concentrations, in central Athens, Greece. Environ. Monit. Assess. 192 (10), 627.

Cohen, A.J., Brauer, M., Burnett, R., Anderson, H.R., Frostad, J., Estep, K., et al., 2017. Estimates and 25-year trends of the global burden of disease attributable to ambient air pollution: an analysis of data from the Global Burden of Diseases Study 2015 [Internet] Lancet 389 (10082), 1907–1918. https://doi.org/10.1016/S0140-6736(17)30505-6. Available from:

Daellenbach, K.R., Uzu, G., Jiang, J., Cassagnes, L.-E., Leni, Z., Vlachou, A., et al., 2020. Sources of particulate-matter air pollution and its oxidative potential in Europe [Internet] Nature 587 (7834), 414–419. https://doi.org/10.1038/s41586-020-2902-8. Available from:

de Jesus, A.L., Rahman, M.M., Mazaheri, M., Thompson, H., Knibbs, L.D., Jeong, C., et al., 2019. Ultrafine particles and PM2.5 in the air of cities around the world: are they representative of each other? [Internet] Environ. Int. 129, 118–135. Available from: http://www.sciencedirect.com/science/article/pii/S0160412019311110.

Delhi, India Population, 2019. Population Stat [Internet]. Available from: https://populationstat.com/india/delhi.

[Internet] Enroth, J., Saarikoski, S., Niemi, J., Kousa, A., Ježek, I., Močnik, G., et al., 2016 May 3. Chemical and physical characterization of traffic particles in four different highway environments in the Helsinki metropolitan area [cited 2020 Apr 21] Atmos. Chem. Phys. 16 (9), 5497–512. Available from: https://www.atmos-chem-phys.net/16/5497/2016/.

Fierz, M., Meier, D., Steigmeier, P., Burtscher, H., 2014. Aerosol measurement by induced currents [Internet] Aerosol. Sci. Technol. 48 (4), 350–357. https://doi.org/10.1080/02786826.2013.875981. Available from:

Fröhlich, R., Cubison, M.J., Slowik, J.G., Bukowiecki, N., Prévôt, A.S.H., Baltensperger, U., et al., 2013. The ToF-ACSM: a portable aerosol chemical speciation monitor with TOFMS detection. Atmos. Meas. Technol. 6 (11), 3225–3241.

[Internet] Gani, S., Bhandari, S., Seraj, S., Wang, D.S., Patel, K., Soni, P., et al., 2019 May 22. Submicron aerosol composition in the world's most polluted megacity: the Delhi Aerosol Supersite study [cited 2020 Apr 21] Atmos. Chem. Phys. 19 (10), 6843–6859. Available from: https://www.atmos-chem-phys.net/19/6843/2019/.

Gaschen, A., Lang, D., Kalberer, M., Savi, M., Geiser, T., Gazdhar, A., et al., 2010 Feb 15. Cellular responses after exposure of lung cell cultures to secondary organic aerosol particles [Internet] Environ. Sci. Technol. 44 (4), 1424–1430. https://doi.org/10.1021/es902261m. Available from:

Habre, R., Zhou, H., Eckel, S.P., Enebish, T., Fruin, S., Bastain, T., et al., 2018. Short-term effects of airport-associated ultrafine particle exposure on lung function and inflammation in adults with asthma. Environ. Int. 118, 48–59. https://doi.org/10.1016/j.envint.2018.05.031.

Hennig, F., Quass, U., Hellack, B., Küpper, M., Kuhlbusch, T.A.J., Stafoggia, M., et al., 2018 Feb 15. Ultrafine and fine particle number and surface area concentrations and daily cause-specific mortality in the ruhr area, Germany, 2009–2014 [Internet] Environ Health Perspect. 126 (2), 27008. https://doi.org/10.1289/EHP2054. Available from:

Henning, S., Ziese, M., Kiselev, A., Saathoff, H., Möhler, O., Mentel, T.F., et al., 2012. Hygroscopic growth and droplet activation of soot particles: uncoated, succinic or

sulfuric acid coated [Internet] Atmos. Chem. Phys. 12 (10), 4525–4537. Available from: https://acp.copernicus.org/articles/12/4525/2012/.
Hinds, W.C., 1999. Aerosol Technology: Properties, Behavior, and Measurement of Airborne Particles, second ed. Wiley-Interscience Publication, New York: Wiley, p. 504.
Hooda, R.K., Hyvärinen, A.-P., Vestenius, M., Gilardoni, S., Sharma, V.P., Vignati, E., et al., 2016. Atmospheric aerosols local–regional discrimination for a semi-urban area in India [Internet] Atmos. Res. 168, 13–23. Available from: http://www.sciencedirect.com/science/article/pii/S0169809515002598.
Human respiratory tract model for radiological protection. A report of a task group of the international commission on radiological protection. Ann. ICRP 24 (1–3), 1994, 1–482.
Hyvärinen, A.P., Lihavainen, H., Komppula, M., Panwar, T.S., Sharma, V.P., Hooda, R.K., et al., 2010. Aerosol measurements at the Gual Pahari EUCAARI station: preliminary results from in-situ measurements. Atmos. Chem. Phys. 10 (15), 7241–7252.
Ihalainen, M., Jalava, P., Ihantola, T., Kasurinen, S., Uski, O., Sippula, O., et al., 2019 Feb 1. Design and validation of an air-liquid interface (ALI) exposure device based on thermophoresis [Internet] Aerosol. Sci. Technol. 53 (2), 133–145. https://doi.org/10.1080/02786826.2018.1556775. Available from:
Ihantola, T., Di Bucchianico, S., Happo, M., Ihalainen, M., Uski, O., Bauer, S., et al., 2020. Influence of wood species on toxicity of log-wood stove combustion aerosols: a parallel animal and air-liquid interface cell exposure study on spruce and pine smoke [Internet] Part. Fibre Toxicol. 17 (1), 27. https://doi.org/10.1186/s12989-020-00355-1. Available from:
Jalava, P.I., Salonen, R.O., Hälinen, A.I., Penttinen, P., Pennanen, A.S., Sillanpää, M., et al., 2006. In vitro inflammatory and cytotoxic effects of size-segregated particulate samples collected during long-range transport of wildfire smoke to Helsinki [Internet] Toxicol. Appl. Pharmacol. 215 (3), 341–353. Available from: http://www.sciencedirect.com/science/article/pii/S0041008X06001062.
[Internet] Järvinen, A., Aitomaa, M., Rostedt, A., Keskinen, J., Yli-Ojanperä, J., 2014 Mar 1. Calibration of the new electrical low pressure impactor (ELPI+) [cited 2018 Jan 10] J. Aerosol Sci. 69, 150–159. https://doi.org/10.1016/j.jaerosci.2013.12.006. Available from:
Jia, B., Gao, M., Zhang, S., Lam Yung, K.K., 2020. Rapid increase in mortality attributable to PM2.5 exposure in India over 1998-2015 [Internet] Chemosphere 128715. Available from: http://www.sciencedirect.com/science/article/pii/S0045653520329131.
Jimenez, J.L., Canagaratna, M.R., Donahue, N.M., Prevot, A.S.H., Zhang, Q., Kroll, J.H., et al., 2009 Dec. Evolution of organic aerosols in the atmosphere. Science 326 (5959), 1525–1529.
Joshi, H., Naja, M., Singh, K.P., Kumar, R., Bhardwaj, P., Babu, S.S., et al., 2016. Investigations of aerosol black carbon from a semi-urban site in the Indo-Gangetic Plain region [Internet] Atmos. Environ. 125, 346–359. https://doi.org/10.1016/j.atmosenv.2015.04.007. Available from:
Keller, J., Wohlleben, W., Ma-Hock, L., Strauss, V., Gröters, S., Küttler, K., et al., 2014. Time course of lung retention and toxicity of inhaled particles: short-term exposure to nano-Ceria [Internet] Arch. Toxicol. 88 (11), 2033–2059. https://doi.org/10.1007/s00204-014-1349-9. Available from:
Keskinen, J., Pietarinen, K., Lehtimäki, M., 1992. Electrical low pressure impactor. J. Aerosol Sci. 23 (4), 353–360.
Kittelson, D.B., 1998. Engines and nanoparticles: a review. J. Aerosol Sci. 29 (5–6), 575–588.
Korhonen, S., Loukkola, K., Portin, H., 2020. Air Quality in the Helsinki Metropolitan Area in 2019. (in Finnish with an abstract in English), Helsinki.
[Internet] Kuula, J., Kuuluvainen, H., Niemi, J.V., Saukko, E., Portin, H., Kousa, A., et al., 2020 Feb 1. Long-term sensor measurements of lung deposited surface area of particulate matter emitted from local vehicular and residential wood combustion sources [cited 2020 Apr 17] Aerosol. Sci. Technol. 54 (2), 190–202. Available from: https://www.tandfonline.com/doi/full/10.1080/02786826.2019.1668909.
Kuuluvainen, H., Rönkkö, T., Järvinen, A., Saari, S., Karjalainen, P., Lähde, T., et al., 2016. Lung deposited surface area size distributions of particulate matter in different urban areas [Internet] Atmos. Environ. 136, 105–113. https://doi.org/10.1016/j.atmosenv.2016.04.019. Available from:
Kuuluvainen, H., Poikkimäki, M., Järvinen, A., Kuula, J., Irjala, M., Dal Maso, M., et al., 2018. Vertical profiles of lung deposited surface area concentration of particulate matter measured with a drone in a street canyon. Environ. Pollut. 241, 96–105.
Lelieveld, J., Evans, J.S., Fnais, M., Giannadaki, D., Pozzer, A., 2015. The contribution of outdoor air pollution sources to premature mortality on a global scale. Nature 525 (7569), 367–371.
Lelieveld, J., Klingmüller, K., Pozzer, A., Pöschl, U., Fnais, M., Daiber, A., et al., 2019. Cardiovascular disease burden from ambient air pollution in Europe reassessed using novel hazard ratio functions. Eur. Heart J. 40 (20), 1590–1596.
Lepistö, T., Kuuluvainen, H., Juuti, P., Järvinen, A., Arffman, A., Rönkkö, T., 2020. Measurement of the human respiratory tract deposited surface area of particles with an electrical low pressure impactor [Internet] Aerosol. Sci. Technol. 1–21. https://doi.org/10.1080/02786826.2020.1745141. Available from:, 0(0).
Li, X., Jin, L., Kan, H., 2019. Air pollution: a global problem needs local fixes. Nature 570 (7762), 437–439.
Lovett, C., Baasiri, M., Atwi, K., Sowlat, M.H., Shirmohammadi, F., Shihadeh, A.L., et al., 2019. Comparison of the oxidative potential of primary (POA) and secondary (SOA) organic aerosols derived from ?-pinene and gasoline engine exhaust precursors [version 2; peer review: 2 approved] [Internet] F1000Research 7 (1031). Available from: http://openr.es/fn2.
Lu, F., Xu, D., Cheng, Y., Dong, S., Guo, C., Jiang, X., et al., 2015. Systematic review and meta-analysis of the adverse health effects of ambient PM2.5 and PM10 pollution in the Chinese population [Internet] Environ. Res. 136, 196–204. https://doi.org/10.1016/j.envres.2014.06.029. Available from:
Marjamäki, M., Keskinen, J., Chen, D.-R., Pui, D.Y.H., 2000. Performance evaluation of the electrical low-pressure impactor [Internet] J. Aerosol Sci. 31, 249–261. Available from: http://www.sciencedirect.com/science/article/pii/S002185029900052X.
[Internet] Moshammer, H., Neuberger, M., 2003 Apr 1. The active surface of suspended particles as a predictor of lung function and pulmonary symptoms in Austrian school children [cited 2020 Apr 17] Atmos. Environ. 37 (13), 1737–1744. Available from: https://www.sciencedirect.com/science/article/pii/S1352231003000736.
Mostafavi, N., Jeong, A., Vlaanderen, J., Imboden, M., Vineis, P., Jarvis, D., et al., 2019. The mediating effect of immune markers on the association between ambient air pollution and adult-onset asthma. Sci. Rep. 9 (1), 1–11.
Mülhopt, S., Dilger, M., Diabaté, S., Schlager, C., Krebs, T., Zimmermann, R., et al., 2016. Toxicity testing of combustion aerosols at the air–liquid interface with a self-contained and easy-to-use exposure system [Internet] J. Aerosol Sci. 96, 38–55. Available from: http://www.sciencedirect.com/science/article/pii/S0021850216300647.
Nair, V.S., Moorthy, K.K., Alappattu, D.P., Kunhikrishnan, P.K., George, S., Nair, P.R., et al., 2007. Wintertime aerosol characteristics over the Indo-Gangetic Plain (IGP): impacts of local boundary layer processes and long-range transport. J. Geophys. Res. Atmos. 112 (13), 1–15.
[Internet] Niemi, J.V., Saarikoski, S., Aurela, M., Tervahattu, H., Hillamo, R., Westphal, D.L., et al., 2009 Feb 1. Long-range transport episodes of fine particles in southern Finland during 1999–2007 [cited 2020 Apr 17] Atmos. Environ. 43 (6), 1255–1264. Available from: https://www.sciencedirect.com/science/article/pii/S135223100801090X.
Obaidullah, M., Bram, S., Verma, V.K., De Ruyck, J., 2012. A review on particle emissions from small scale biomass combustion [Internet] Int. J. Renew. Energy Resour. 2 (1), 147–159. Available from: http://www.ijrer.net/index.php/ijrer/article/view/147.
Oberdörster, G., 1996. Significance of particle parameters in the evaluation of exposure-dose-response relationships of inhaled particles [Internet] Inhal. Toxicol. 8 (Suppl. L), 73–89. Available from: https://www.scopus.com/inward/record.uri?eid=2-s2.0-0030308101&partnerID=40&md5=6586fe5aace37ad374f1deaaeeae5573.
Oberdörster, G., Oberdörster, E., Oberdörster, J., 2005. Nanotoxicology: an emerging discipline evolving from studies of ultrafine particles. Environ. Health Perspect. 113 (7), 823–839.
Ouf, F.-X., Sillon, P., 2009 Jun 19. Charging efficiency of the electrical low pressure impactor's corona charger: influence of the fractal morphology of nanoparticle aggregates and uncertainty analysis of experimental results [Internet] Aerosol. Sci. Technol. 43 (7), 685–698. https://doi.org/10.1080/02786820902878245. Available from:
Pañella, P., Casas, M., Donaire-Gonzalez, D., Garcia-Esteban, R., Robinson, O., Valentín, A., et al., 2017. Ultrafine particles and black carbon personal exposures in asthmatic and non-asthmatic children at school age. Indoor Air 27 (5), 891–899.
Park, M., Joo, H.S., Lee, K., Jang, M., Kim, S.D., Kim, I., et al., 2018. Differential toxicities of fine particulate matters from various sources [Internet] Sci. Rep. 8 (1), 17007. https://doi.org/10.1038/s41598-018-35398-0. Available from:
Patel, S., Leavey, A., Sheshadri, A., Kumar, P., Kandikuppa, S., Tarsi, J., et al., 2018. Associations between household air pollution and reduced lung function in women and children in rural southern India. J. Appl. Toxicol. 38 (11), 1405–1415.
Pelucchi, C., Negri, E., Gallus, S., Boffetta, P., Tramacere, I., La Vecchia, C., 2009. Long-term particulate matter exposure and mortality: a review of European epidemiological studies. BMC Publ. Health 9, 1–8.
Pirjola, L., Niemi, J.V., Saarikoski, S., Aurela, M., Enroth, J., Carbone, S., et al., 2017. Physical and chemical characterization of urban winter-time aerosols by mobile measurements in Helsinki, Finland. Atmos. Environ. 158, 60–75.
Pohjola, M.A., Kousa, A., Kukkonen, J., Härkönen, J., Karppinen, A., Aarnio, P., et al., 2002. The spatial and temporal variation of measured urban PM10 and PM2.5 in the helsinki metropolitan area. Urban Air Qual — Recent Adv. 189–201.
[Internet] Population, 2019. Statistics Finland. Available from: https://www.stat.fi/tup/suoluk/suoluk_vaesto_en.html.
[Internet] Puthussery, J.V., Zhang, C., Verma, V., 2018 Oct 19. Development and field testing of an online instrument for measuring the real-time oxidative potential of ambient particulate matter based on dithiothreitol assay [cited 2020 May 29] Atmos. Meas. Technol. 11 (10), 5767–5780. Available from: https://www.atmos-meas-tech.net/11/5767/2018/.
Puthussery, J.V., Singh, A., Rai, P., Bhattu, D., Kumar, V., Vats, P., et al., 2020 May 18. Real-time measurements of PM2.5 oxidative potential using a dithiothreitol assay in Delhi, India [Internet] Environ. Sci. Technol. Lett. 7 (7), 504–510. https://doi.org/10.1021/acs.estlett.0c00342. Available from:
Raatikainen, T., Hyvärinen, A.-P.P., Hatakka, J., Panwar, T.S., Hooda, R.K., Sharma, V. P., et al., 2014. The effect of boundary layer dynamics on aerosol properties at the Indo-Gangetic plains and at the foothills of the Himalayas [Internet] Atmos. Environ. 89, 548–555. https://doi.org/10.1016/j.atmosenv.2014.02.058. Available from:
Reche, C., Viana, M., Brines, M., Perez, N., Beddows, D., Alastuey, A., et al., 2015 Jun. Determinants of aerosol lung-deposited surface area variation in an urban environment. Sci. Total Environ. 517, 38–47.
Rissler, J., Nordin, E.Z., Eriksson, A.C., Nilsson, P.T., Frosch, M., Sporre, M.K., et al., 2014 Jun 3. Effective density and mixing state of aerosol particles in a near-traffic urban environment [Internet] Environ. Sci. Technol. 48 (11), 6300–6308. https://doi.org/10.1021/es5000353. Available from:
Ritchie, H., 2019. Outdoor air pollution [Internet] Our World Data. Available from: https://ourworldindata.org/outdoor-air-pollution.
Rönkkö, T., Timonen, H., 2019. Overview of sources and characteristics of nanoparticles in urban traffic-influenced areas. J. Alzheimers Dis. 72 (1), 15–28.

Rönkkö, T., Kuuluvainen, H., Karjalainen, P., Keskinen, J., Hillamo, R., Niemi, J.V., et al., 2017. Traffic is a major source of atmospheric nanocluster aerosol [Internet] Proc. Natl. Acad. Sci. Unit. States Am. 114 (29), 7549–7554. Available from: http://www.pnas.org/lookup/doi/10.1073/pnas.1700830114.

Saffari, A., Daher, N., Shafer, M.M., Schauer, J.J., Sioutas, C., 2014 Jul 1. Global perspective on the oxidative potential of airborne particulate matter: a synthesis of research findings [Internet] Environ. Sci. Technol. 48 (13), 7576–7583. https://doi.org/10.1021/es500937x. Available from:

Samet, J.M., Dominici, F., Curriero, F.C., Coursac, I., Zeger, S.L., 2000 Dec 14. Fine particulate air pollution and mortality in 20 U.S. Cities, 1987–1994 [Internet] N. Engl. J. Med. 343 (24), 1742–9. Available from: http://www.nejm.org/doi/abs/10.1056/NEJM200012143432401.

Schmid, O., Stoeger, T., 2016. Surface area is the biologically most effective dose metric for acute nanoparticle toxicity in the lung [Internet] J. Aerosol. Sci. 99, 133–143. https://doi.org/10.1016/j.jaerosci.2015.12.006. Available from:

Song, C., He, J., Wu, L., Jin, T., Chen, X., Li, R., et al., 2017. Health burden attributable to ambient PM2.5 in China. Environ. Pollut. 223, 575–586. https://doi.org/10.1016/j.envpol.2017.01.060.

Stoeger, T., Reinhard, C., Takenaka, S., Schroeppel, A., Karg, E., Ritter, B., et al., 2006. Instillation of six different ultrafine carbon particles indicates a surface area threshold dose for acute lung inflammation in mice. Environ. Health Perspect. 114 (3), 328–333.

Surawski, N.C., Miljevic, B., Ayoko, G.A., Roberts, B.A., Elbagir, S., Fairfull-Smith, K.E., et al., 2011 Jul 1. Physicochemical characterization of particulate emissions from a compression ignition engine employing two injection technologies and three fuels [Internet] Environ. Sci. Technol. 45 (13), 5498–5505. https://doi.org/10.1021/es200388f. Available from:

Swietlicki, E., Hansson, H.-C., Hämeri, K., Svenningsson, B., Massling, A., Mcfiggans, G., et al., 2008 Jan 1. Hygroscopic properties of submicrometer atmospheric aerosol particles measured with H-TDMA instruments in various environments—a review [Internet] Tellus B 60 (3), 432–469. https://doi.org/10.1111/j.1600-0889.2008.00350.x. Available from:

Teinilä, K., Aurela, M., Niemi, J.V., Kousa, A., Petäjä, T., Järvi, L., et al., 2019. Concentration variation of gaseous and particulate pollutants in the helsinki city centre — observations from a two-year campaign from 2013–2015. Boreal Environ. Res. 24 (September), 115–136.

[Internet] Timonen, H., Saarikoski, S., Tolonen-Kivimäki, O., Aurela, M., Saarnio, K., Petäjä, T., et al., 2008 Sep 26. Size distributions, sources and source areas of water-soluble organic carbon in urban background air [cited 2020 Apr 17] Atmos. Chem. Phys. 8 (18), 5635–47. Available from: https://www.atmos-chem-phys.net/8/5635/2008/.

Timonen, H., Aurela, M., Carbone, S., Saarnio, K., Saarikoski, S., Mäkelä, T., et al., 2010. High time-resolution chemical characterization of the water-soluble fraction of ambient aerosols with PILS-TOC-IC and AMS [Internet] Atmos. Meas. Technol. 3 (4), 1063–1074. Available from: https://amt.copernicus.org/articles/3/1063/2010/.

Tissari, J., 2008. Fine Particle Emissions from Residential Wood Combustion.

Tiwari, S., Srivastava, A.K., Bisht, D.S., Parmita, P., Srivastava, M.K., Attri, S.D., 2013. Diurnal and seasonal variations of black carbon and PM2.5 over New Delhi, India: influence of meteorology [Internet] Atmos. Res. 125–126, 50–62. https://doi.org/10.1016/j.atmosres.2013.01.011. Available from:

Tran, P.T.M., Ngoh, J.R., Balasubramanian, R., 2020. Assessment of the integrated personal exposure to particulate emissions in urban micro-environments: a pilot study. Aerosol. Air Qual. Res. 20 (2), 341–357.

Verma, V., Fang, T., Xu, L., Peltier, R.E., Russell, A.G., Ng, N.L., et al., 2015 Apr 7. Organic aerosols associated with the generation of reactive oxygen species (ROS) by water-soluble PM2.5 [Internet] Environ. Sci. Technol. 49 (7), 4646–4656. https://doi.org/10.1021/es505577w. Available from:

Virtanen, A., Rönkkö, T., Kannosto, J., Ristimäki, J., Mäkelä, J.M., Keskinen, J., et al., 2006. Winter and summer time size distributions and densities of traffic-related aerosol particles at a busy highway in Helsinki. Atmos. Chem. Phys. 6 (9), 2411–2421.

Vu, T.V., Zauli-Sajani, S., Poluzzi, V., Harrison, R.M., 2018. Factors controlling the lung dose of road traffic-generated sub-micrometre aerosols from outdoor to indoor environments [Internet] Air Qual. Atmos. Health 11 (6), 615–625. https://doi.org/10.1007/s11869-018-0568-2. Available from:

Wang, C.-F., Chang, C.-Y., Tsai, S.-F., Chiang, H.-L., 2005. Characteristics of road dust from different sampling sites in northern taiwan [Internet] J. Air Waste Manag. Assoc. 55 (8), 1236–1244. https://doi.org/10.1080/10473289.2005.10464717. Available from:

Wang, L., Slowik, J.G., Tripathi, N., Bhattu, D., Rai, P., Kumar, V., et al., 2020. Source characterization of volatile organic compounds measured by PTR-ToF-MS in Delhi, India [Internet] Atmos. Chem. Phys. Discuss. 2020, 1–27. Available from: https://www.atmos-chem-phys-discuss.net/acp-2020-11/.

Zhao, G., Chen, Y., Hopke, P.K., Holsen, T.M., Dhaniyala, S., 2017. Characteristics of traffic-induced fugitive dust from unpaved roads [Internet] Aerosol. Sci. Technol. 51 (11), 1324–1331. https://doi.org/10.1080/02786826.2017.1347251. Available from: